PHYSICAL REVIEW B **81**, 100403(R) (2010)

Intrinsic damping of spin waves by spin current in conducting two-dimensional systems

J. Gómez,[1] F. Perez,[1] E. M. Hankiewicz,[2] B. Jusserand,[1] G. Karczewski,[3] and T. Wojtowicz[3]
[1]*Institut des Nanosciences de Paris, CNRS/Université Paris VI, Paris, France*
[2]*Institut für Theoretische Physik und Astrophysik, Universität Würzburg, Germany*
[3]*Institute of Physics, Polish Academy of Sciences, Warsaw, Poland*
(Received 5 February 2010; published 2 March 2010)

Angle-resolved magneto-Raman scattering has been performed on spin-polarized two-dimensional electron gas embedded in $Cd_{1-x}Mn_xTe$ quantum wells to explore the intrinsic damping of propagating spin-wave modes with in plane momentum q. The damping rate η follows a quadratic law $\eta=\eta_0+\eta_2 q^2$ due to losses in the spin current driven by the magnetization in qualitative agreement with Phys. Rev. B **78**, 020404(R) (2008). As a consequence, the propagation length of a spin wave in a conducting system has an intrinsic maximum of importance for spin-wave-based spintronics.

DOI: 10.1103/PhysRevB.81.100403 PACS number(s): 75.45.+j, 75.30.Ds, 76.30.−v, 78.30.−j

Avoiding dissipation of spin currents in the context of spin-based electronics has become an important challenge today. Indeed, in devices using spin-polarized currents,[1] the spin of carriers is displaced together with their charge. This results in joule dissipation. Pure spin currents (PSCs) without net charge current have been recently proposed in nonmagnetic materials with spin-orbit interaction.[2] However, they suffer from an intrinsic damping, the so-called spin Coulomb drag (SCD),[3,4] which results from the friction between carriers with antiparallel spins. The SCD is very efficient in semiconductors where PSCs involve longitudinal (with respect to the spin-quantization axis) spin degrees of freedom. An alternative would be to make use of transverse spin degrees of freedom, naturally good candidate for pure spin information transport. For example, spin waves in ferromagnets may be the means to transmit and modify a logical information.[5] They are also the elemental components of transverse PSCs. In this frame, understanding the intrinsic limitations of spin-wave propagation is crucial. Recently, the attention to this topic has been drawn in Ref. 6, where it was found that a spin wave of momentum q in a spin-polarized conducting system had an intrinsic damping proportional to q^2.

We have performed angle-resolved electronic resonant Raman-scattering (ERRS) experiments on a two-dimensional (2D) conducting spin-polarized system to evidence the q^2 intrinsic damping of propagating spin-wave modes. We also completed the theory of Ref. 6 by exact dynamics considerations. The damping rate we found experimentally varies as q^2 as predicted in Ref. 6, but additional corrections were necessary to match quantitatively the data without fitting parameters.

We studied high mobility two-dimensional electron gases (2DEGs) embedded in $Cd_{1-x}Mn_xTe/Cd_{0.8}Mg_{0.2}Te$ quantum wells.[7] Such systems have been recently introduced as a test-bed system for spin excitations of the spin-polarized 2DEG (SP2DEG).[8,9] Indeed, the *s-d* exchange coupling of conduction electron with localized electrons of the Mn atoms provide a giant Zeeman energy[10] to the 2DEG:

$$Z(B,T)=\bar{x}N_0\alpha_e\langle S_z(B,T)\rangle-|g_e|\mu_B B, \tag{1}$$

where N_0 is the cation sites density, α_e is the exchange coupling between the conduction electron of the well and the localized electrons on Mn impurities ($N_0\alpha_e=-0.22$ eV).[10] $\langle S_z(B,T)\rangle$ is the thermal average spin of a single Mn atom given by the modified Brillouin function, $\bar{x}$ is the effective Mn concentration (for low x, $\bar{x}\simeq x$), g_e is the normal electron g factor, and μ_B is the Bohr magneton ($\mu_B>0$). In order to keep alloy disorder low and high electron mobilities ($\mu\sim 10^5$ cm^2 V s), x remained below 1% and the electron sheet density n_{2D} ranged in between 1.5 and 4×10^{11} cm^{-2}. Depending on the Mn nominal concentration xN_0 and n_{2D}, the maximum spin-polarization degree $\zeta=(n_\uparrow-n_\downarrow)/n_{2D}$ can reach 80% for a magnetic field B below 4 T, such that, when B is applied parallel to the quantum well plane, the Landau orbital quantization is kept negligible. Therefore, such SP2DEG are "artificial" conducting paramagnet having the spin-polarization degree of a conducting ferromagnet. Moreover, semiconductor quantum wells exhibit well-defined optical resonances which allow ERRS measurements to be performed.[11] ERRS is a powerful tool to access wave-vector resolution of the spin excitation spectrum.[8] Over the last decades, general knowledge on electron gases low-energy excitations has been considerably improved by ERRS study of high mobility unpolarized 2DEG.[12] We claim that the SP2DEG system investigated here is able to provide general knowledge on spin waves in spin-polarized conducting systems, in particular to the subject here: the q^2 damping.

We start with the theoretical description of the intrinsic damping and consider the Hamiltonian of the above spin-polarized 2DEG:

$$\hat{H}_{\mathrm{SP2DEG}}=\hat{H}_{\mathrm{Kin}}+\hat{H}_{\mathrm{Zeeman}}+\hat{H}_{\mathrm{Coulomb}}, \tag{2}$$

where $\hat{H}_{\mathrm{Kin}}+\hat{H}_{\mathrm{Zeeman}}=\Sigma_{\mathbf{k},\sigma}(E_{\mathbf{k}}+\sigma Z)c^+_{\mathbf{k},\sigma}c_{\mathbf{k},\sigma}$ and $E_{\mathbf{k}}=\hbar^2k^2/2m^*$ is the kinetic energy of the single electron state $|\mathbf{k}\sigma\rangle$ with in-plane wave-vector $\mathbf{k}$ and spin $\sigma=\pm\frac{1}{2}$. Z is the Zeeman energy given by Eq. (1). $c^{(+)}_{\mathbf{k}\sigma}$ are creation-annihilation operators. Spin waves are transverse precession modes of the magnetization described by the operators $\hat{S}_{+,\mathbf{q}}=\int\int\hat{\mathbf{S}}_+(\mathbf{r})e^{-i\mathbf{q}\cdot\mathbf{r}}d^2r$, space Fourier transform of the transverse spin-density $\hat{\mathbf{S}}_+(\mathbf{r})$. As $\hat{S}_{+,\mathbf{q}}=\Sigma_{\mathbf{k}}c^+_{\mathbf{k}-\mathbf{q},\uparrow}c_{\mathbf{k},\downarrow}$, a magnetization can also be seen as a coherent superposition of individual spin-flip electron-hole pairs: $c^+_{\mathbf{k}-\mathbf{q},\uparrow}c_{\mathbf{k},\downarrow}|0\rangle$. In presence,

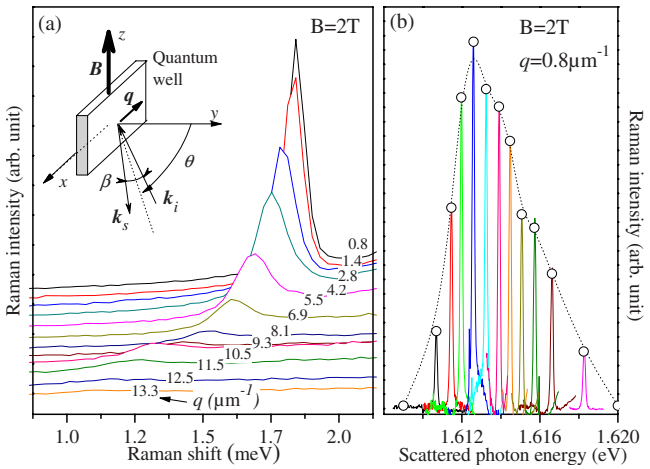

FIG. 1. (Color online) (a) Typical crossed polarized Raman spectra obtained on sample A at $B=2$ T and for different values of q. The single Raman line is the SFW. A sketch of the scattering geometry shows the angles definition. Incoming photon is polarized parallel to $\mathbf{B}(\pi)$, while the scattered one is polarized perpendicular to $\mathbf{B}(\sigma)$. (b) Spectra obtained by shifting the laser wavelength. Amplitude variations of the Raman line reveal the optical resonance width.

of a perturbing rotating magnetic field $b_+(\mathbf{r},t)=b_{+\mathbf{q}\omega}e^{i\mathbf{q}\cdot\mathbf{r}-i\omega t}$, the equation of motion for the magnetization $\mathfrak{m}_{+\mathbf{q}\omega}=\langle\hat{S}_{+,\mathbf{q}}\rangle_\omega$ with ω and $\mathbf{q}$ Fourier components writes exactly as

$$\omega\mathfrak{m}_{+\mathbf{q}\omega}=\omega_0\mathfrak{m}_{+\mathbf{q}\omega}+\mathbf{q}\cdot\langle\hat{J}_{+,\mathbf{q}}\rangle_\omega+M_0g_e\mu_Bb_{+\mathbf{q}\omega}. \tag{3}$$

In Eq. (3), $Z=\hbar\omega_0$ and $M_0=\langle\hat{S}_{z,\mathbf{q}=0}\rangle_0$ is the equilibrium 2DEG magnetization. The first term in the right-hand side of Eq. (3) arises from $[\hat{S}_{+,\mathbf{q}},\hat{H}_{\text{Zeeman}}+\hat{H}_{\text{Coulomb}}]$. The second term in the rhs of Eq. (3) is the discussed effect and is the commutator $[\hat{S}_{+,\mathbf{q}},\hat{H}_{\text{Kin}}]=\Sigma_{\mathbf{k}}(E_{\mathbf{k}}-E_{\mathbf{k}-\mathbf{q}})c^+_{\mathbf{k}-\mathbf{q},\uparrow}c_{\mathbf{k},\downarrow}$, written in terms of $\hat{J}_{+,\mathbf{q}}=\frac{\hbar}{m^*}\Sigma_{\mathbf{k}}(\mathbf{k}-\frac{\mathbf{q}}{2})c^+_{\mathbf{k}-\mathbf{q},\uparrow}c_{\mathbf{k},\downarrow}$, the Fourier transform of the transverse spin-current density. Hence, if $\mathbf{q}\neq0$, the kinetic Hamiltonian couples the magnetization to the spin current. One is left with exploring the dynamics of the spin current. Despite its collective character, this quantity is not conserved by Coulomb, neither it is by the kinetic part because of the spread of velocities of individual pairs. This makes its dynamics governed by individual dynamics of $c^+_{\mathbf{k}-\mathbf{q},\uparrow}c_{\mathbf{k},\downarrow}$. The latter experiences scattering due to disorder but also scattering due to Coulomb which couples the single electron-hole pair $c^+_{\mathbf{k}-\mathbf{q},\uparrow}c_{\mathbf{k},\downarrow}$ with multiple electron-hole pairs having the same total spin (+1). The spin Coulomb drag theory[3] describes to leading order the efficiency of multipair scattering. Among scatterings, individual pairs are sensitive to a local magnetic field, addition of the external one and the Coulomb exchange-correlation field due to other individual pairs. The latter field brings the theoretical contribution of this work, which was not taken into account in Ref. 6. The spin-current equation of motion writes then (to first order in $b_{+\mathbf{q}\omega}$) as

$$\langle\hat{J}_{+,\mathbf{q}}\rangle_\omega=-\mathbf{q}\tilde{\sigma}_\perp\left(\frac{1}{2}g_e\mu_Bb_{+\mathbf{q}\omega}-U\mathfrak{m}_{+\mathbf{q}\omega}\right), \tag{4}$$

where $\tilde{\sigma}_\perp=-\frac{\langle\langle\hat{J}_{+,\mathbf{q}};\hat{J}_{-,-\mathbf{q}}\rangle\rangle_\omega}{\omega-\omega_0}$ is the spin conductivity linking $\langle\hat{J}_{+,\mathbf{q}}\rangle_\omega$ to the gradient of the magnetic field,[6] which is enhanced by the local exchange-correlation field $-U\mathfrak{m}_{+\mathbf{q}\omega}$. U is the transverse local-field factor. In the local spin-density approximation, $U=-\frac{2}{M_0}\frac{\partial E_{xc}}{\partial M_0}$, where E_{xc} is the exchange-correlation part of the ground-state energy.[9] This local-field factor is also responsible for the Zeeman energy enhancement:[13] $Z^*=\hbar\omega_0^*=Z-UM_0$. Hence, it is clear from Eqs. (3) and (4) that any loss in the spin current (imaginary contribution in $\tilde{\sigma}_\perp$) introduces a damping of the magnetization precession, proportional to q^2. The resulting Gilbert damping α is given by

$$\alpha=\frac{\hbar\omega_0^2}{2M_0}\lim_{\omega\to0}\frac{\text{Im}\,\chi_+}{\omega} \tag{5}$$

$$=-\frac{q^2\hbar}{4M_0}\left[\sigma_\perp+\sigma'_\perp\omega_0-\frac{2M_0}{\hbar}U\left(\sigma'_\perp+2\frac{\sigma_\perp}{\omega_0}\right)\right] \tag{6}$$

$$=\frac{q^2\hbar}{2m^*|\zeta|}\frac{\omega_0^*}{\omega_0}\frac{3\tau}{(\omega_0^*\tau)^2+1}\left[\frac{\omega_0^*}{\omega_0}-\frac{(\omega_0^*\tau)^2+1/3}{(\omega_0^*\tau)^2+1}\right], \tag{7}$$

where $\chi_+=\frac{\mathfrak{m}_{+\mathbf{q}\omega}}{g_e\mu_Bb_{+\mathbf{q}\omega}}$ is the spin-susceptibility, $\sigma_\perp=\text{Im}\,\tilde{\sigma}_\perp(0)$ and $\sigma'_\perp=\lim_{\omega\to0}\frac{\text{Im}\,\tilde{\sigma}_\perp(\omega)}{\omega}$. Compared to Ref. 6, the second, third, and fourth terms in Eq. (6) are the additional contributions introduced here. Obviously the last two are due to the Coulomb local field, while the second term is due to dynamical properties of the spin conductivity. Further considerations on $\tilde{\sigma}_\perp$ show that disorder and Coulomb scattering give additive imaginary contributions in the spin current–spin current reponse[6] $\langle\langle\hat{J}_{+,\mathbf{q}};\hat{J}_{-,-\mathbf{q}}\rangle\rangle_\omega$. Therefore, the scattering time τ introduced in Eq. (7) is given by $\frac{1}{\tau}=\frac{1}{\tau_{dis}}+\frac{1}{\tau_{ee}}$, $\frac{1}{\tau_{dis}}$, and $\frac{1}{\tau_{ee}}$ are, respectively, the disorder and transverse-spin Coulomb drag scattering rates.

Evidence of this universal q^2 behavior has been performed in the high mobility SP2DEG described above. Since, the well-defined spin-wave modes has been successfully observed in these quantum wells,[8] this material is a perfect candidate to investigate the damping. The sketch on Fig. 1 depicts the experimental geometry: the external magnetic field ($\mathbf{B}$) is applied in the z direction parallel to the quantum well plane and the average angle θ of the incoming and backscattered light wave vectors with respect to the normal direction can be tuned to make the in-plane Raman transferred wave vector $q=\frac{4\pi}{\lambda}\cos\frac{\beta}{2}\sin\theta$ vary in the range $0<q<16$ μm^{-1}, $\beta\simeq5°$ and λ is the incoming light wavelength.

When the polarizations of the incoming and scattered photons are crossed, the Raman spectrum is determined by the transverse spin-susceptibility spectrum $\text{Im}\,\chi_+(q,\omega)$. This is always true when out of resonance. In resonance, however, it remains valid if q is small compared to wave vectors of electrons involved in optical processes (typically greater than the Fermi wave vector k_F) and when the intermediate state

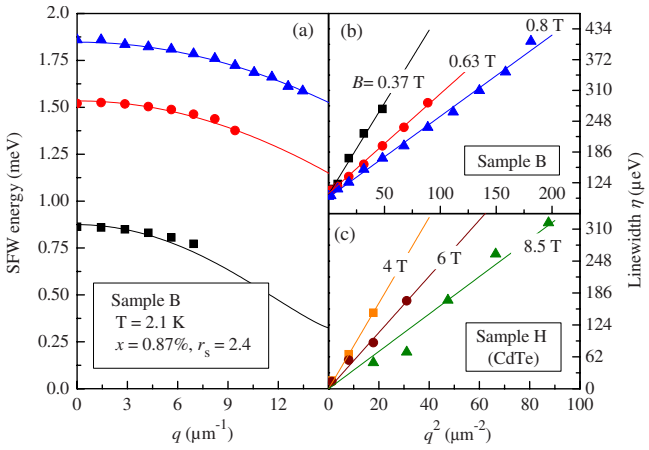

FIG. 2. (Color online) (a) Typical SFW energy and (b) linewidth q dependence obtained on sample B (x=0.87%, r_s=2.4) for B=0.37, 0.63, and 0.8 T. In agreement with Eqs. (8) and (9) the data follow a parabolic behavior. (c) Linewidth q dependence obtained on CdTe sample H.

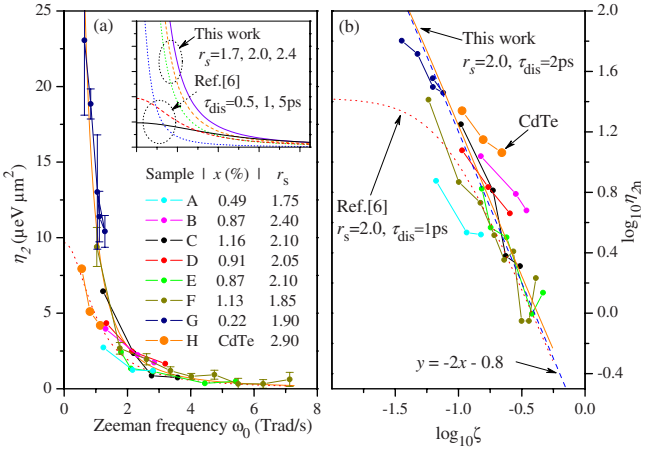

FIG. 3. (Color online) q^2-damping and spin polarization. (a) η_2 is plotted as a function of ω_0. Symbols are data obtained on samples with various Mn (x) and electron (r_s) concentrations. Concentrations are measured as in Ref. 13. Lines are calculated η_2: using Eq. (7) with r_s=2 and τ_{dis}=2 ps (full line), using Ref. 6 with r_s=2 and τ_{dis}=1 ps (dotted line). The insert shows variations in Eq. (7) with r_s (upper curve is lower r_s) and variations of Ref. 6 with τ_{dis} (flatter curve is lower τ_{dis}). (b) Check of the power-law behavior: $\eta_{2n}=\eta_2/\frac{\hbar^2}{2m^*}$ is plotted as a function of the spin polarization ζ in a $\log_{10}$ frame. Lines corresponds to calculated η_{2n} from (a). All data curves are parallel to $y=-2x$.

lifetime is shorter than the one of the excitation considered. The former condition is immediately fulfilled as q remains much smaller than typical $k_F \sim 150\ \mu\text{m}^{-1}$.

In Fig. 1(a), we have plotted typical crossed polarized Raman spectra obtained for increasing q and fixed external magnetic field at superfluid He bath temperature ($T \sim 2$ K). These spectra present a clear dispersive Raman line associated to the spin-flip wave (SFW) excitation of the SP2DEG.[13] In Fig. 1(b), we show the resonant behavior of the Raman peak when tuning the laser wavelength across the optical resonance. This shows how the resonance width is 20 times larger than the SFW line in the Raman spectra. Hence, we can consider that Raman spectra give access to Im $\chi_+(q,\omega)$ and extract from these data both the SFW energy ($\hbar\omega_{SFW}$) and the line width η q dependence. As shown in Fig. 2(a) the former is well reproduced by the formula[9] below:

$$\hbar\omega_{SFW} = Z - \frac{1}{|\zeta|}\frac{Z}{Z^* - Z}\frac{\hbar^2}{2m^*}q^2, \tag{8}$$

when m^*=0.105m_e is the CdTe conduction electron effective mass. This provides another confirmation for the identification of the Raman line. Following previous assessments, we have extracted the linewidth of the Raman line after background subtraction and deconvolution with the spectrometer response (Voigt profile of apparent FWHM 62 μeV) to get the damping rate of magnetization modes. The deconvoluted linewidth η of the Raman line is plotted in Fig. 2(b) as a function of q^2 for the same conditions as the dispersions plotted in Fig. 2(a). It shows that, in the explored range of wave vectors ($q \ll k_F$), the linewidth q dependence is very well reproduced by a parabolic function:

$$\eta = \eta_0 + \eta_2 q^2. \tag{9}$$

In Eq. (9), η_0 gives the homogenous mode (q=0) damping and η_2 is inferred to be linked to the q^2 damping of Eq. (5): $\eta_2 = 2\hbar\omega_0\alpha/q^2$. Indeed, η_2 has obviously a strong magnetic field dependence. We may ask if the presence of Mn impurities can be the cause of η_2? It is already known that Mn spin fluctuations damp the homogeneous mode.[14] But, in our samples, the typical Mn average distance $\bar{d} \sim 0.4$ nm is far smaller than the minimum magnetization wavelength probed in the Raman experiment ($q\bar{d} \ll 1$). Hence, Mn damping is expected to be constant in the explored range of q and not present in η_2. We confirmed by carrying the same measurements on a CdTe quantum well (without Mn). Figure 2(c) shows that the same q^2 law has been found and that η_2 has the same order of magnitude. Without Mn, the Zeeman energy is much lower and requires higher fields, this reduces the range of explored spin polarization. Consequently, we claim that the Mn damping is, here, present in η_0 and that η_2 originates from the general behavior described above. Let us compare the experimental η_2 with the theoretical one.

Figure 3 shows the behavior of the q^2 damping η_2 with the polarization or equivalently with the Zeeman pulsation ω_0. η_2 determined on all the studied samples is compared with the calculations of Eqs. (7)–(9) and Ref. 6. The accuracy of the measurements is not able to separate variations of η_2 with the electron density within the small range explored here (r_s=5 nm/$\sqrt{\pi n_{2D}} \in [1.7, 2.4]$). But within the experimental error, all the CdMnTe data follows the same power law even if the Mn concentration varies like 1:5. This confirms that the observed phenomenon is not due to the presence of Mn impurities. CdTe data need additional treatment because of mass renormalization due to high magnetic fields. This is out of the scope. We will concentrate on the average behavior of CdMnTe data. First, the behavior for $\omega_0 \to 0$ is impossible to explore below 1.0 T rad/s (0.65 meV) as such pulsations are beyond the rejection of the spectrometer. But

in the range of explored pulsations, as shown in Fig. 3(a) the average curve is very well reproduced by Eqs. (7)–(9) when taking a disorder scattering time $\tau_{dis} \sim 2$ ps. For such a time scale, densities, and experimental conditions, the spin-Coulomb drag coefficient $\frac{1}{\tau_{ee}}$ is always smaller than 15 ns^{-1} and has negligible impact on measurements. However, enhancement of both the Zeeman energy ($Z^* \geq Z$) and the transverse field due to the Coulomb local exchange field are clearly needed to make the theory of Ref. 6 match the experiment. Insert of Fig. 3(a) shows how, even when varying the disorder time τ_{dis}, Eq. (20) of Ref. 6 does not reproduce the data. These conclusions are clearer when plotting $\eta_{2n} = \eta_2 / \frac{\hbar^2}{2m^*}$ as a function of the spin polarization ζ in a log-log frame as shown in Fig. 3(b). Indeed, when $\omega_0 \geq 1$ T rad/s and for $r_s \sim 2$, the Zeeman enhancement $\omega_0^*/\omega_0 \sim 2$, so $(\omega_0^* \tau_{dis})^2 \gg 1$ and η_{2n} becomes

$$\lim_{\omega_0^* \tau_{dis} \gg 1} \eta_{2n} \simeq \frac{1}{\zeta^2} \frac{1}{E_F} \frac{\hbar}{\tau} 3 \left[\frac{\omega_0^*}{\omega_0} - 1 \right]. \tag{10}$$

Comparing Eq. (10) and Fig. 3(b), the $1/\zeta^2$ behavior is fulfilled by the data even for the lowest measurable frequencies in agreement with η_{2n} calculated by Eq. (7). On the contrary, the $1/\zeta^2$ behavior requests higher frequencies to appear in Eq. (20) of Ref. 6. This confirms that spin-current dynamics is determined by individual pair dynamics for which the relevant precession pulsation is ω_0^* and not ω_0. Moreover, the individual spin-flip scattering time has been probed by ERRS in the same conditions[13] from $q=0$ spectra. At $q=0$, the energies of individual pairs are degenerate to Z^* and presents a well-defined peak in Raman spectra. Processing the linewidth of this peak with the same procedure gives a time in between 1.2 and 1.8 ps in very good agreement with the present determination of τ_{dis}.

In conclusion, we have demonstrated both experimental and theoretically that, in conducting systems, transverse propagating spin waves with momentum $q \neq 0$ carry a spin current, which despite its collective character is governed by single particle dynamics, where both disorder and spin-Coulomb drag play a role. Both mechanisms induce losses in the spin current which damp the magnetization mode with a rate proportional to q^2. The form of this damping is intrinsically linked to the kinetic motion of the spin carriers. Consequently, in the context of magnonics[5] performed in 2D or three-dimensional (3D) ferromagnetic metals, the propagation length l_{prop} of a spin wave in a conducting system has to be optimized: assuming a group velocity $v_g = \beta q$ and a damping rate similar to Eq. (9), then l_{prop} reaches its maximum $\beta\hbar / \sqrt{\eta_0 \eta_2}$ for $q_{\max} = \sqrt{\eta_0 / \eta_2}$.

The authors would like to thank M. Combescot and G. Vignale for fruitful discussions as well as ANR grant GOSPININFO, German Grant No. HA 5893/1-1 and Polish MNiSW Grant No. 202 054 32/1198 for financial supports.

[1] A. Fert and S. F. Lee, Phys. Rev. B **53**, 6554 (1996).
[2] S. Murakami, N. Nagaosa, and S.-C. Zhang, Science **301**, 1348 (2003).
[3] I. D'Amico and G. Vignale, Phys. Rev. B **62**, 4853 (2000); E. M. Hankiewicz and G. Vignale, J. Phys.: Condens. Matter **21**, 253202 (2009).
[4] C. P. Weber, N. Gedik, J. E. Moore, J. Orenstein, J. Stephens, and D. D. Awschalom, Nature **437**, 1330 (2005).
[5] D. S. Deng, X. F. Jin, and R. Tao, Phys. Rev. B **66**, 104435 (2002); V. V. Kruglyak and R. J. Hicken, J. Magn. Magn. Mater. **306**, 191 (2006).
[6] E. M. Hankiewicz, G. Vignale, and Y. Tserkovnyak, Phys. Rev. B **78**, 020404(R) (2008).
[7] G. Karczewski, J. Jaroszyń, A. Barcz, M. Kutrowski, T. Wojtowicz, and J. Kossut, J. Cryst. Growth **184-185**, 814 (1998).
[8] B. Jusserand, F. Perez, D. R. Richards, G. Karczewski, T. Wojtowicz, C. Testelin, D. Wolverson, and J. J. Davies, Phys. Rev. Lett. **91**, 086802 (2003).
[9] F. Perez, Phys. Rev. B **79**, 045306 (2009).
[10] J. A. Gaj, R. Planel, and G. Fishman, Solid State Commun. **29**, 435 (1979).
[11] G. Abstreiter, M. Cardona, and A. Pinczuk, *Light Scattering in Solids IV* (Springer, New York, 1984).
[12] G. F. Giuliani and G. Vignale, *Quantum Theory of the Electron Liquid* (Cambridge University Press, Cambridge, 2005).
[13] F. Perez, C. Aku-leh, D. Richards, B. Jusserand, L. C. Smith, D. Wolverson, and G. Karczewski, Phys. Rev. Lett. **99**, 026403 (2007).
[14] S. A. Crooker, J. J. Baumberg, F. Flack, N. Samarth, and D. D. Awschalom, Phys. Rev. Lett. **77**, 2814 (1996).